

## ELECTRICAL CHARACTERIZATION OF HYDROTHERMALLY SYNTHESIZED METAL OXIDE NANOWIRES WITH REGARD TO OXYGEN ADSORPTION/DESORPTION THERMODYNAMICS

<sup>1</sup>Petr SMISITEL, <sup>2</sup>Helena SIMUNKOVA, <sup>1,2</sup>Ondrej CHMELA, <sup>3</sup>Martha CLAROS,  
<sup>1,4</sup>Stella VALLEJOS, <sup>1,2</sup>Jaromir HUBALEK

<sup>1</sup>Central European Institute of Technology (CEITEC), Brno University of Technology, Czech Republic, EU,  
[smisitel@vutbr.cz](mailto:smisitel@vutbr.cz)

<sup>2</sup>Department of Microelectronics, Faculty of Electrical Engineering and Communication (FEEC), Brno University of Technology, Czech Republic, EU, [simunkova@vutbr.cz](mailto:simunkova@vutbr.cz)

<sup>3</sup>Escuela de Ingeniería Química, Pontificia Universidad Católica de Valparaíso, Valparaíso, Chile

<sup>4</sup>Instituto de Microelectrónica de Barcelona, IMB-CNM (CSIC), Spain, EU

<https://doi.org/10.37904/nanocon.2022.4583>

### Abstract

Self-assembled metal oxide MnO<sub>2</sub> nanowires (NWs) were hydrothermally synthesized and electrically characterized. The nanowires were from 3 to 10 μm long and from 20 to 100 nm in diameter. The nanowires were suspended in water and deposited on gold interdigitated electrode (IDE) chip using dielectrophoresis (DEP) to align them perpendicularly across the electrodes. Screening of the MnO<sub>2</sub> material properties, such as semiconductor type, vacancies concentration and relative permittivity was performed by means of impedance and Mott-Schottky analyses. The conductivity was measured both in synthetic air and in nitrogen ambient. The tests consisted in measuring resistivity of the NWs in relation to temperature of the bottom-placed heater under the IDE chip. The temperature went from room temperature up to 300 °C. The resistivity changes were observed accounting for oxygen reduction on the NWs surface as the electrons were moving from the NWs to the oxygen. The resistivity was explored at a constant current arrangement test. Overall, we observed changes in the electrical properties of the wires upon oxygen adsorption, such as activation energy. Therefore, in future experiments, we might also explore the effect of other gases on the NW's electrical properties, e.g., ethanol, H<sub>2</sub>, NO<sub>2</sub>.

**Keywords:** MnO<sub>2</sub> nanowires, dielectrophoresis, gas sensing, resistivity, Mott-Schottky analysis

### 1. INTRODUCTION

Single NW devices seems to be a promising way to improve sensitivity and selectivity of metal-oxide (MOX) gas sensors thanks to high surface to volume ratio. MOX gas sensors rely on reactions of detected gas with oxygen adsorption layer formed on the NW surface in the air. As the reactions are often thermally activated the MOX sensors are typically heated by external heater causing relatively high power consumption. A future motivation of our study is a precise temperature control including a self-heating effect. Moreover, good understanding of oxygen adsorption layer formation and its influence on NW electrical properties is also highly desirable. In the air, oxygen species (O<sub>2</sub>, O<sup>-</sup>, O<sup>2-</sup>) get adsorbed on the nanowire surface influencing the NW electrical properties. Oxygen acts as an oxidizing agent. By trapping electrons from the NW, the oxygen negative surface charge leads to upwards band bending and formation of electron lateral depletion layer (around the NW surface) in n-type MOX and hole accumulation layer in p-type MOX. The result is the formation of core-shell configuration: e.g., in p-type NW the core has the highest resistance while the main conducting channel is the shell formed by hole accumulation layer with increased free charge carrier concentration [1]. The oxygen adsorption might be disturbed by air pollutants. Therefore, synthetic air (SA) with constant composition is applied to eliminate a possible interference with air pollutants, as well as to maintain a stable

humidity and create the same conditions as for measurements in nitrogen (namely the same constant flow of gas in measurement chamber). The second set of measurements was done using nitrogen as inert atmosphere. The purpose is to eliminate the oxygen adsorption providing so a reference measurement with no electron lateral depletion/hole accumulation layer allowing the evaluation of oxygen adsorption influence on NWs electrical properties. Additionally, impedance and Mott-Schottky analyses were performed to corroborate a type and vacancies concentration of the semiconductor. By polarizing the IDE / MnO<sub>2</sub> (metal/semiconductor) interface, a potential barrier either emerges or an existing one might narrow or broaden because of a direct potential  $V$  applied for a certain time. Considering a p-type semiconductor, a negative space charge layer arises on the side of positive potential due to a depletion (repulsion) of the positively charged carriers. The depletion layer (frontal contact depletion = on the interface with IDEs, not the same as lateral depletion) or let's say the space charge layer might be determined by the linear relationship between the inverse second power of the space charge capacitance  $C_{SC}^{-2}$  and the applied bias  $V$ , which is expressed by the Mott-Schottky equation [2]:

$$C_{SC}^{-2} = \frac{2}{\epsilon_r \epsilon_0 e N_A} (V_{FB} - V - \frac{kT}{e}) \quad (1)$$

where  $e$  is the electron charge,  $N_A$  is the acceptor density in the semiconductor (cm<sup>-3</sup>),  $V$  is the applied voltage, and  $V_{FB}$  is the flat-band voltage. The Mott-Schottky equation is a valid tool to determine the type of a semiconductor and the acceptor density, as well as the flat-band voltage. The acceptor or donor density can be calculated from the slope of the  $C_{SC}^{-2}$  vs.  $V$  curve, and the flat-band voltage  $V_{FB}$  can be determined by extrapolation to  $C_{SC} = 0$ . For a p-type semiconductor response  $C_{SC}^{-2}$  vs.  $V$  should be linear with a negative slope that is inversely proportional to the acceptor concentration  $N_A$  in the film. For an n-type semiconductor the slope should be positive. Relative permittivity  $\epsilon_r$  of the hydrothermally prepared nanowires might be estimated by knowing a frontal contact depletion layer thickness, as well as the space charge capacitance at a certain direct potential applied. Mott-Schottky analysis can be applied to a system of fixed vacancies (dopants) concentration [2]. Therefore, the  $C_{SC}$  versus  $V$  was measured at a high rate scanning of about 600 mV/sec, in order to avoid a change in the dimension or vacancy profile of the film (i.e.  $N_A$  cannot be a function of  $V$ ). Moreover, no dependence on frequency is expected from Mott-Schottky theory [2], therefore all  $C/V$  analyses were carried out at high frequencies 10 kHz - 1 MHz.

## 2. EXPERIMENTAL

### 2.1. Dielectrophoretic preparation of aligned MnO<sub>2</sub> nanowires

A drop of MnO<sub>2</sub> NWs diluted water solution was placed on the ID electrodes connected to alternating voltage (sinusoidal with 5  $V_{PP}$ , 9 MHz) for approx. 3 minutes. Afterwards, the drop was removed by compressed air. The nanowires long enough to connect the electrodes were captured while the majority of the shorter NW were removed with the rest of the drop leaving clean electrodes with 24 single-nanowire connections. Further pre-treatment was done directly in a flowing gas chamber. The sample was connected to constant 0.1  $\mu$ A current flow and slowly heated up to 275 °C, where it was held for 15 minutes (until the resistance was stabilized). The result was approx. one order drop in resistance thanks to a strengthening of the NWs to the electrode contact.

### 2.2. Resistivity vs. temperature analysis

Resistivity in dependence on temperature was measured by using a custom build setup. Sample was placed on ceramic heater located in an enclosed chamber providing a slow constant flow of gas - either synthetic air (SA) or nitrogen was used. Direct measurements of NWs temperature were not possible, the readout from the bottom-placed heater was used. Sample was connected to the source of constant current (KEITHLEY 2401 Source Measure Unit) and temperature was driven from room temperature (25 °C) up to 300 °C and back to 25 °C again. The temperature was recorded in 10 degrees increments every 5 minutes. A stabilization time for reaching an adsorption/desorption equilibrium per temperature was hence 5 minutes. Both heating and cooling

proceeded at the same rate. Before experiments in nitrogen, the setup equipment had to be pure of oxygen. Even after flushing the apparatus with nitrogen, oxygen keeps desorbing from inner walls of measuring chamber, tubing, sample itself, etc. Therefore at least 24 hours flushing is necessary to reach good quality oxygen free atmosphere. As a direct control of NWs temperature was not available, we needed to eliminate the self-heating effect that would cause difference between real NW temperature and value measured on the heater. Therefore, low probing current 0.1  $\mu\text{A}$  was chosen, meaning the Joule heating power was lower than 1 nW per nanowire.

### 2.3. C/V, Mott-Schottky analysis

The impedance spectrum analyses were carried out dry (without electrolyte), performed using  $\mu\text{AutolabIII}$  potentiostat/FR analyzer (Metrohm). In all cases, a 10 mV sinusoidal excitation signal was employed to interrogate the capacitance. C/V behavior was determined in a direct bias range +/- 5V. Diverse formation times were tested: 60, 120 and 360 s, whereas the formation potential was always +5 V. Consequently, Mott-Schottky plots  $1/C_{SC}^2$  vs.  $V$  were performed. The analyses were carried out in a frequency range of 1 MHz-10 kHz. Moreover, a broad range (1 MHz - 0.1 Hz) impedance analysis was performed as well. According to an impedance data simulation, the frontal contact depletion layer capacitance shows a CPE-like distribution behavior rather than that of a pure capacitor. The frequency dispersion is generally attributed to a capacitance dispersion (frequency-dependent capacitance) expressed in terms of a constant-phase element (CPE) [3]. The impedance of CPE is defined as follows [4]:

$$Z_{CPE} = \frac{1}{Q(j\omega)^\alpha} \quad (2)$$

where,  $Q$  (in  $\text{F cm}^{-2} \text{ s}^{-\alpha}$ ) and  $\alpha$  are the CPE parameters.  $\alpha$  equals the slope of the log-log imaginary impedance plot vs frequency. Both parameters, as well as  $R$  from the equation below, were obtained by regression of a simple equivalent ( $R$ ,  $Q$ ) circuit implemented by an impedance analysis software (a graphical method). The so called effective equivalent capacitance  $C_{eff}$  value was then extracted from the parameters  $\alpha$ ,  $Q$  and  $R$  using the Hsu and Mansfeld formula [5]:

$$C_{eff} = Q^{1/\alpha} R^{(1-\alpha)/\alpha} \quad (3)$$

For better clarity:  $C = C_{eff} = C_{SC}$  in our study.

## 3. RESULTS

### 3.1. Synthesis and characterization of the $\text{MnO}_2$ nanowires

The nanowires were obtained by the hydrothermal synthesis method presented elsewhere [6]. The product of the hydrothermal synthesis is a brown powder with high density of nanowires as shown in SEM image (**Figure 1(a)**), in which several well-defined nanowires with smooth and uniform surface are observed. The synthesis procedure was repeatable usually obtaining the same yield (~ 55 %) and nanostructure morphology. The structures are crystalline, and their diameter and length vary from ~20 nm to ~100 nm and from ~3 to ~10  $\mu\text{m}$ , respectively. The crystallinity was corroborated elsewhere [6] by a high-resolution TEM image and a XRD diffraction pattern recorded for the synthesized powder. The presence of intense diffraction peaks in the XRD pattern indicates that the obtained product is well crystallized.

### 3.2. Dielectrophoretic preparation of aligned $\text{MnO}_2$ nanowires

Separated and alone-standing  $\text{MnO}_2$  nanowires were aligned perpendicularly to the ID gold electrodes by means of dielectrophoretic technique, see **Figure 1(b)** (described in the experimental part). After the preparation the nanowires were observed by scanning electron microscopy (SEM), see **Figure 1(c)**. In total, there were 24 nanowires standing alone and connecting the two parallel ID electrodes all over the sample.

The nanowires surroundings were clean from impurities, such as nanowires flocks, or short nanowires crossing the long ones. The measurement area was therefore well defined, given by the length and diameter of the 24 single nanowires.

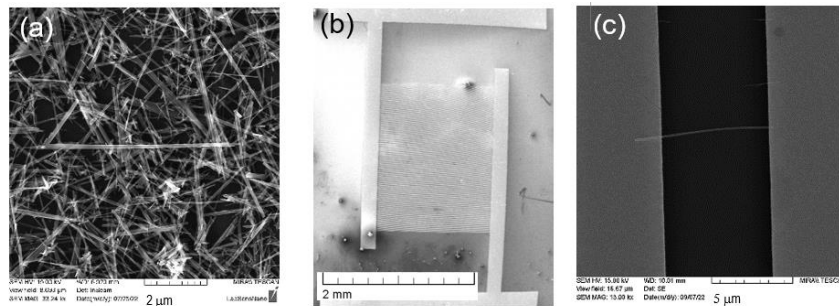


**Figure 1** Scanning electron micrographs of: (a) MnO<sub>2</sub> nanowires, (b) gold interdigitated electrodes IDEs, (c) single nanowire aligned between two ID electrodes.

### 3.3. Resistivity thermal analysis

The resistance was measured in temperature range from room temperature to 300 °C and the influence of oxygen adsorption was evaluated.

Basic equation derived from concentration of thermally activated free charge carriers

$$\rho = \rho_0 e^{E_a/kT} \quad (4)$$

describes the thermal resistivity dependence in semiconductors, where  $\rho_0$  is a material constant,  $E_a$  activation energy and  $k$  is Boltzman constant. This model is too simple to fully describe our measurement as there are other effect involved (oxygen adsorption, self-heating effect, Shottky contacts), however this simple equation well fits the data above aprox. 120 °C (the operation range of metal oxide gas sensors), see **Figure 2(a)**. This well-predictable behaviour is beneficial for potential sensing applications. Keeping in mind that MnO<sub>2</sub> is a p-type semiconductor, the adsorbed oxygen creates surface acceptor states resulting in lowering the MnO<sub>2</sub> activation energy (see **Table 1**), as well as overall increase of hole concentration under the surface (formation of hole accumulation layer in the outer shell-part of the MnO<sub>2</sub> NWs). Comparing the two experimental setups - concerning the synthetic air and the nitrogen ambients - we might conclude that the resistivity decreases in synthetic air compared to nitrogen, **Figure 2(a)**. The overall result is decrease of the resistivity caused by the oxygen adsorption, which is typical for p-type MOX.

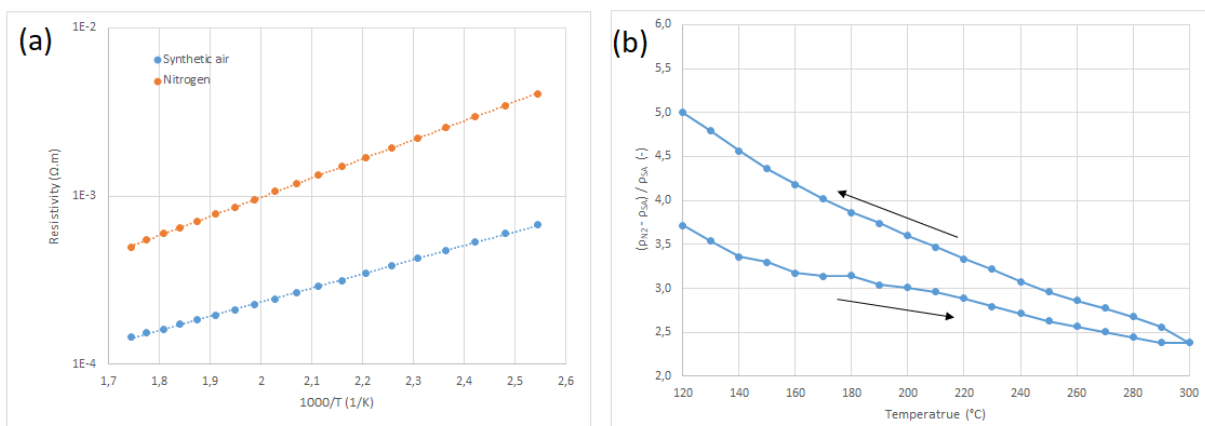


**Figure 2** (a) The Arrhenius plot of resistivity vs. temperature range 120 - 300 °C fitted to equation (4), (b) relative resistivity change caused by removal of adsorbed oxygen both during heating and cooling.

**Table 1** Parameters obtained by fitting the equation (4) to resistivity data in range 120 - 300 °C

	0.1 $\mu$ A, SA	0.1 $\mu$ A, N <sub>2</sub>
$\rho_0$ ( $10^{-6}$ $\Omega$ .m)	4.9	11.1
$E_a$ (eV)	0.17	0.23

The effect of oxygen adsorption on NWs resistance and its temperature dependence can be better estimated from relative resistance change between  $\rho_{N_2}$  and  $\rho_{SA}$ , see **Figure 2(b)**. The relative resistivity difference is decreasing with temperature, which can be explained by lower equilibrium concentration of adsorbents at higher temperatures [7]. Measurements were done both during heating and cooling. A significant hysteresis can be seen, with higher resistivity difference (corresponding to higher concentration of adsorbed oxygen) during the cooling compared to heating meaning that 5 minutes stabilization time was not sufficient to reach the equilibrium adsorbents concentration.

### 3.4. C/V, Mott-Schottky analysis

The relationship of the reciprocal capacitance square vs bias (Mott-Schottky analysis) of the MnO<sub>2</sub> NWs was employed to estimate a frontal contact depletion layer capacitance which had arisen during a formation by a direct potential V. Moreover, by this method we had approved that the MnO<sub>2</sub> NWs are a p-type semiconductor. Additionally, acceptors (probably Mn metal vacancies) concentration, depletion layer thickness and permittivity were estimated as well. To be reproducible with the C/V characterization, we had searched for a formation conditions (potential, time) of our nanowires. At a formation potential a rise of a quasi-stable depletion layer thickness assuming a rectangular distribution with a quasi-constant charge would be expected. At first, we applied a constant bias of +5 V for 60 seconds, which was further determined as insufficient. The positive charge carrier's depletion on the interface with the positively charged contact was not completed yet. Therefore, we prolonged the formation time up to 6 minutes. During the formation, the current passing through the structure did not change significantly, being about  $7 \cdot 10^{-7}$  A, which is about 30 nA passing through one nanowire (24 NWs in total). After 360 seconds, we had obtained a depletion layer stable enough, which was approved by the C/V analysis, see **Figure 3**. The last formation step resulted in an almost constant shape of the Mott-Schottky plot in the bias range of +5 V to -1 V. The space charge acts as a pure capacitor at that moment and conditions. Increasing the potential towards negative values, a depletion layer thickness would narrow, and the space charge capacitance would increase. The linear part of the Mott-Schottky plot accounts for a semiconductive behaviors. A descend of the  $1/C^2$  vs. V plot was observed in the negative bias range from -1 V to -5 V. The negative slope accounts for a p-type semiconductor and it is inversely proportional to the acceptor concentration  $N_A$  in the film.

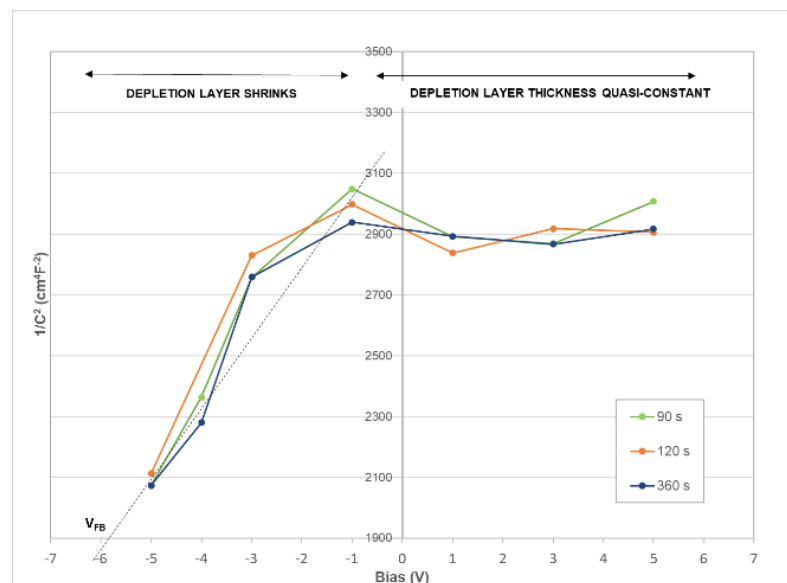


**Figure 3** Mott-Schottky plots at various stabilization times (90, 120 and 360 s). Measured at high frequency range 10 kHz - 1 MHz. Capacitance obtained via a graphical simulation of the impedance data.

The acceptor concentration  $N_A$  (metal vacancies) might be calculated from the Mott-Schottky plot slope according to the equation (1). For that we need to know the  $\text{MnO}_2$  relative permittivity. The relative permittivity was determined from the depletion layer capacitance, as well as from depletion layer thickness according to following equation:

$$\varepsilon_r = \frac{d}{A} \cdot \frac{C}{\varepsilon_0} \quad (5)$$

where,  $d$  is a nanowire diameter,  $A$  is a nanowire area,  $C$  is depletion layer capacitance and  $\varepsilon_0$  is vacuum permittivity. The depletion layer thickness was estimated by SEM analysis after finishing the  $C/V$  experiments. Most probably, due to the potential formation trials, the nanowires got burned at the end of the  $C/V$  experiments. The current after burning the NWs off descended down the  $10^{-12}$  A and the potential across them increased. Moreover, the SEM images showed that the nanowires burned near to the IDE electrode surface, see **Figure 4**. The nanowire might burn just at the end of the depletion layer. Considering the entire nanowire length, the place where the negatively charged depletion layer ends has a highest resistivity towards minority charge carriers (electrons) compared to the rest nanowire volume. The burning spot accounts for a place with the highest resistivity. The distance between the spot and IDE was about 730 nm. This length might be a thickness of the depletion layer. Consequently, the relative permittivity was calculated from equation (5) leading to about  $1.6 \cdot 10^7$ . The acceptor concentration  $N_A$  (metal vacancies) was evaluated in the range of  $1.8 \cdot 10^{22}$  -  $3.9 \cdot 10^{22} \text{ cm}^{-3}$ . The higher the slope, the lower the concentration. The highest acceptor concentration was evaluated after the longest time of stabilization (360 s). To get a preciser acceptor concentration a more detailed analysis would be needed. Capacitances were determined from the high frequency range analyses 1 MHz-10 kHz (140 pF, i.e., 117 F/g). The capacitances were in good conjunction with other studies [8,9].

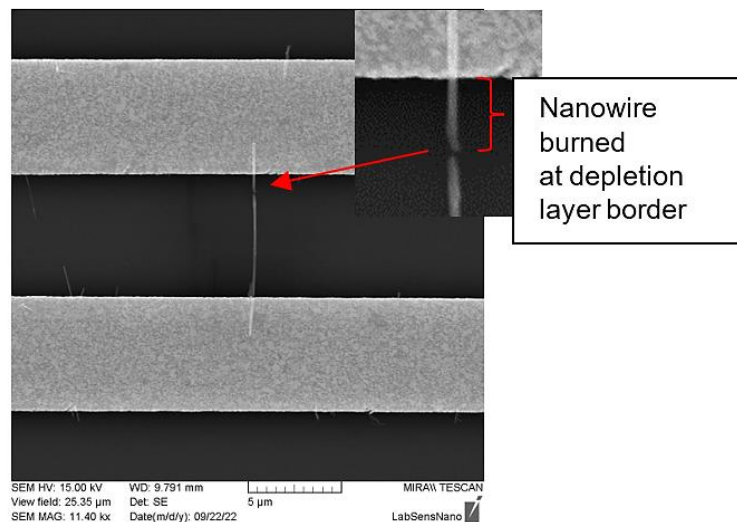


**Figure 4** SEM micrograph and a detail of single  $\text{MnO}_2$  nanowire after burning off.

#### 4. CONCLUSION

In general, the study provides an overall electrical characterization of the hydrothermally synthesized  $\text{MnO}_2$  nanowires. We approved that the  $\text{MnO}_2$  nanowires are a p-type semiconductor, whereas permittivity and vacancies concentration were estimated. Resistivity of the NWs was tested in a reference synthetic air system in comparison to nitrogen ambient. The resistivity difference of the NWs in the two ambiances caused by oxygen adsorption was evaluated leading to its changes in relation to temperature variations. The knowledge gained in this study will serve as a reference platform for future gas sensing experiments.

## ACKNOWLEDGEMENTS

**The work was done under the Czech Grant Agency project no. 22-14886S  
and project no. CZ.02.2.69 / 0.0 / 0.0 / 19\_073 / 0016948 under Quality Internal Grants of BUT.**

## REFERENCES

- [1] KIM, H.-J., LEE, J.-H. Highly sensitive and selective gas sensors using p-type oxide semiconductors: Overview. *Sensors and Actuators B: Chemical*. 2014, vol. 192, pp. 607-627.
- [2] MORRISON, S. *Electrochemistry at Semiconductor and Oxidized Metal Electrodes*. 2. print. New York: Plenum Press, 1984.
- [3] JORCIN, J.-B., ORAZEM, M.E., PEBERE, N., TRIBOLLET, B. CPE analysis by local electrochemical impedance spectroscopy. *Electrochimica Acta*. 2006, vol. 51, pp. 1473-1479.
- [4] LVOVICH, V.F. *Impedance Spectroscopy*. New Jersey: John Wiley & Sons, Inc., 2012.
- [5] HIRSCHORN, M.E., ORAZEM, M.E., TRIBOLLET, B., VIVIER, V., FRATEUR, I., MUSIANI, M. Determination of effective capacitance and film thickness from constant-phase-element parameters. *Electrochimica Acta*. 2010, vol. 55, pp. 6218-6227.
- [6] CLAROS, M., KUTA, J., EL-DAHSHAN, O. MICHALIČKA, J., JIMENEZ, Y.P., VALLEJOS, S. Hydrothermally synthesized MnO<sub>2</sub> nanowires and their application in Lead (II) and Copper (II) batch adsorption. *Journal of Molecular Liquids*. 2021, vol. 325, pp. 115203.
- [7] IWAMOTO, M., YODA, Y., YAMAZOE, N., SEIYAMA, T. Study of metal oxide catalysts by temperature programmed desorption. 4. Oxygen adsorption on various metal oxides. *The Journal of Physical Chemistry*. 1978, vol. 82, pp. 2564-2570.
- [8] ZHU, J, HE, J. Facile Synthesis of Graphene-Wrapped Honeycomb MnO<sub>2</sub> Nanospheres and Their Application in Supercapacitors. *ACS Applied Materials & Interfaces*. 2012, vol. 4, pp. 1770-1776.
- [9] KIM, M., HWANG, Y., KIM, J. Super-capacitive performance depending on different crystal structures of MnO<sub>2</sub> in graphene/MnO<sub>2</sub> composites for supercapacitors. *Journal of Material Science*. 2013, vol. 48, pp. 7652-7663.